ADVANCED PHOTONICS RESEARCH
www.adpr-journal.com

Vacuum–Sublimable Ionic Yellow Phosphorescent Iridium(III) Complexes with Broad Emission for White Electroluminescence

Peng Tao, Xiao-Kang Zheng, Yuk-Ki Lee, Guo-Liang Wang, Fei-Yang Li, Zi-Kang Li, Qiang Zhao,* Yan-Qin Miao,* and Wai-Yeung Wong**

The exploration of efficient yellow emitters featuring broad emission band plays an essential role for the complementary-color-based white organic light-emitting devices (OLEDs). Herein, two new yellow ionic iridium(III) complexes (Ir1 and Ir2) having excellent sublimation ability are designed and prepared by the incorporation of chlorine-modified 2-phenylquinoline ligand and introduction of bulky counter ion. At room temperature, these ionic iridium(III) complexes show bright yellow phosphorescence in both solid and solution states due to the presence of bulky counter ion. They share the same emission wavelength (538 and 573 nm as the emission shoulder) with extremely high quantum yields (as high as 0.91) in Ar-saturated CH_2Cl_2. Notably, those complexes also exhibit very broad full width at half maximum (FWHM) (up to 100 nm) attributed to almost the same intensities of emission maximum and shoulder, making them excellent candidates for white electroluminescence. The as-prepared yellow OLEDs show high external quantum efficiency (*EQE*) of 11.6% and broad FWHM of 105 nm. The two-color-based white OLED is prepared with peak *EQE* of 9.2%, the 1931 CIE coordinate of (0.29, 0.31), and color rendering index of 79, proving that these new ionic iridium(III) complexes show a great potential for white electroluminescence.

1. Introduction

Phosphorescent molecular materials have become the most popular emitters due to their effective use of triplet excitons formed in organic light-emitting devices (OLEDs), which can greatly boost the device efficiency.[1–5] As an important class of phosphorescent materials, the yellow phosphors can be potentially used for designing high-quality complementary-color-based white electroluminescence.[5a,6–11] The exploration of high-performance yellow phosphors is of great significance for developing complementary-color-based white OLEDs.[5a,12–15]

Ionic iridium(III) complexes are emerging as a promising category of phosphorescent materials because of their rich emissive excited states and facile synthesis, which have been widely used in the fields of biosensors, bioimaging, cancer therapy, and light-emitting electrochemical cells.[16–20] Different from the neutral iridium(III) complexes, the ionic ones rarely served as the emitters in vacuum-evaporated OLEDs.[21–25] Wong and coworkers prepared the first OLED using the ionic iridium(III) complexes with hexafluorophosphate (PF_6^-) as the counter ion by vacuum thermal evaporation method.[21] Due to the strong electrostatic interaction between the iridium(III) cation and the small PF_6^- of the aforementioned iridium(III) emitters, the sublimation ability of the ionic iridium(III) emitters bearing PF_6^- is usually poor, resulting in the low device efficiency. Duan and coworkers designed some

P. Tao, Y.-K. Lee, Z.-K. Li, W.-Y. Wong
Department of Applied Biology and Chemical Technology and Research Institute for Smart Energy
The Hong Kong Polytechnic University
Hung Hom, Hong Kong, P. R. China
E-mail: pengtao@polyu.edu.hk; wai-yeung.wong@polyu.edu.hk

P. Tao, W.-Y. Wong
Shenzhen Research Institute
The Hong Kong Polytechnic University
Shenzhen 518057, P. R. China

The ORCID identification number(s) for the author(s) of this article can be found under https://doi.org/10.1002/adpr.202100115.

DOI: 10.1002/adpr.202100115

X.-K. Zheng, F.-Y. Li, Q. Zhao
State Key Laboratory of Organic Electronics and Information Displays & Jiangsu Key Laboratory for Biosensors
Institute of Advanced Materials (IAM) & Institute of Flexible Electronics (Future Technology)
Nanjing University of Posts and Telecommunications (NUPT)
Nanjing 210023, P. R. China
E-mail: iamqzhao@njupt.edu.cn

G.-L. Wang, Y.-Q. Miao
Key Laboratory of Interface Science and Engineering in Advanced Materials of Ministry of Education
Taiyuan University of Technology
Taiyuan 030024, P. R. China
E-mail: miaoyanqin@tyut.edu.cn

ionic iridium(III) emitters by rationally selecting the counterions, and they found that the sublimation ability and the luminescent quantum yields of the ionic iridium(III) emitters can be remarkably enhanced by incorporating more bulky counter ions.[22,26] Attributed to the improved sublimation ability, the performances of devices based on these sublimable ionic iridium(III) emitters are also increased.[23] Nevertheless, the device efficiency of ionic iridium(III) emitter-based OLEDs is still lagging far behind that of the neutral iridium(III) emitter-based ones.[24,27] From the viewpoint of the molecular design, there is still plenty of room for improving the device performance of ionic iridophosphors.

Recently, a series of neutral iridium(III) emitters with broad yellow emission based on 2-phenylquinoline derivatives by rational ligand modification were developed for highly efficient yellow and white OLEDs.[5a,28] The external quantum efficiency (*EQE*) of yellow devices incorporating the chlorine-modified phenylquinoline-based neutral iridium(III) emitters can be up to 24%.[28] Encouraged by the aforementioned results, in this work, we aim to further explore the potential utilization of the chlorine-modified 2-phenylquinoline ligand in designing high-performance new ionic iridium(III) emitters for preparing the yellow and white OLEDs. We select the newly developed cyclometalating ligand 2-(4-chloro-3-(trifluoromethyl)phenyl)-4-methylquinoline to prepare two yellow ionic iridium(III) phosphors. The trifluoromethyl group and chlorine atom are introduced into the ligand for manipulating the emission energies and photoluminescence (PL) quantum efficiencies of the ionic iridium(III) phosphors in both solid and solution states. Moreover, the incorporation of trifluoromethyl group may also enhance the sublimation ability of the ionic iridium(III) emitters suitable for vacuum thermal evaporation. Moreover, the use of chlorine atom may also enhance the structural stability of the iridium(III) cation relative to the fluorine-containing counterpart under the device operation.[5b–5f] 4,4′–Dimethyl-2,2′-bipyridine and 4,4′-di-*tert*-butyl-2,2′-bipyridine served as the ancillary ligand. The tetrakis(3,5-bis(trifluoromethyl)phenyl)borate was selected as the bulky counter ion. The two as-prepared ionic iridium(III) complexes show bright yellow luminescence with extremely high photoluminescent quantum yields (up to 0.91) in both solution and solid states. These complexes were further used to prepare yellow OLEDs showing broad full width at half maximum (FWHM) of 105 nm and peak *EQE* of 11.6%. Finally, using complex **Ir2**, the two-color-based white device was prepared with the peak *EQE* of 9.2%, the color render index (CRI) of 79, and the 1931 CIE coordinate of (0.29, 0.31).

2. Results and Discussion

2.1. Synthesis and Characterizations

The chemical structures of ionic iridium(III) phosphors and their synthetic routes are shown in **Figure 1**a. The cyclometalating ligand and the μ-chloro-bridged iridium(III) dimer were prepared using the reported methods.[28] The target ionic emitters **Ir1** and **Ir2** were synthesized in two steps. First, the complex bearing chloride ion was obtained by stirring μ-chloro-bridged iridium(III) dimer with 2,2′-bipyridine derivative in the mixed solvents of CH_3OH and CH_2Cl_2 at 50 °C under N_2. After completing the reaction, the residues were obtained by removing the solvent under reduced pressure, and then dissolved it in an appropriate amount of CH_3OH. Then, the aqueous solution containing the stoichiometric sodium tetrakis[3,5-bis(trifluoromethyl)phenyl]borate was injected slowly into stirring CH_3OH

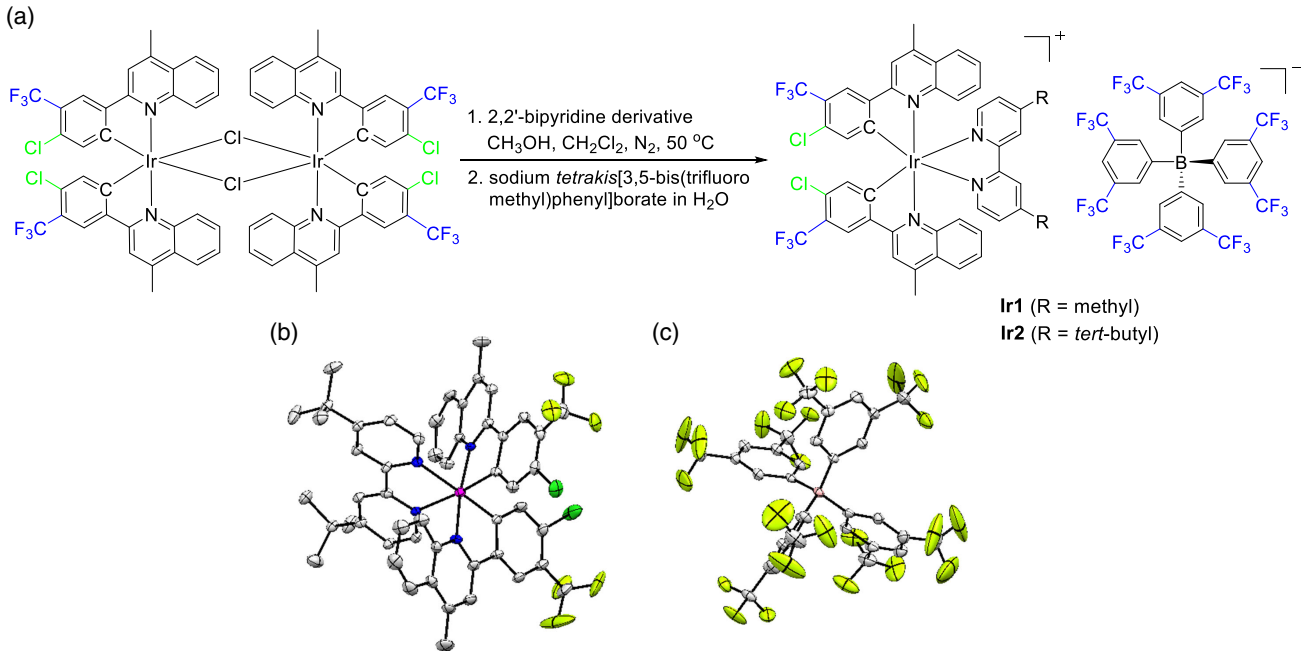

Figure 1. a) Synthesis and chemical structures of ionic iridium(III) complexes; b) ORTEP plots of the cation and c) counter ion of the ionic complex **Ir2** (CCDC no. 2 055 690). Note: the carbon atom in gray, iridium atom in scarlet, nitrogen atom in blue, fluorine atom in chartreuse, chlorine atom in green, and boron atom in pink.

solution of the complex bearing chloride ion at room temperature. The target complexes can precipitate out of the solution immediately.

Quite different from chloride ion-based ionic iridium(III) complexes, it is interesting that the exchange of chloride ion of the iridium(III) complexes with tetrakis[3,5-bis(trifluoromethyl)phenyl]borate ion remarkably reduces the adsorption ability of these target complexes on silica gel during purfication, proving that the bulky organic ion has great influence on the adsorption power of the ionic iridium(III) phosphors. These complexes are obtained in high yield (over 80%). The characterizations of their chemical structures were conducted by nuclear magnetic resonance (NMR) spectrum and mass spectrum (MS). The existence of tetrakis[3,5-bis(trifluoromethyl)phenyl]borate ion can be clearly proved by both ^{1}H and ^{19}F NMR. Taking the complex **Ir1** as an example, as shown in the Supporting Information, the signals of the fluorines (−68.25 ppm and −68.59 ppm) from two different kinds of CF_3 groups were also clearly observed, and the signals of the protons (7.69 ppm, 8H), (7.43 ppm, 4H) from the tetrakis[3,5-bis(trifluoromethyl) phenyl]borate ion well matched with the signal of the protons (2.89 ppm, 6H) from methyl groups on the cyclometalating ligands, supporting the formation and the purity of the ionic phosphors.

The single crystals of complex **Ir2** for X-ray analysis were successfully crystallized from the solvents of acetone and methanol. The Oak Ridge Thermal-Ellipsoid Plot Program (ORTEP) plots of the cation and counter ion of the ionic complex **Ir2** are shown in Figure 1b,c. Table S1, Supporting Information, lists the crystallographic data for **Ir2**. The bond lengths of two C—Cl bonds are 1.73 Å and 1.74 Å, consistent with the reported C_{aryl}—Cl bond length.[28,29] The distance between the adjacent metal center of the cations is 12.8 Å (**Figure 2**a), which is larger than that of the neutral ones based on the same cyclometalating ligand (e.g., 10.20 Å and 11.46 Å).[28] The enhancement of the distance is the result of the incorporation of the bulky counter ion. The distance between the adjacent boron center and metal center of the complex **Ir2** is 9.27 Å (Figure 2a). In addition, no π–π interaction is observed in the crystal structure of complex **Ir2** because of the incorporation of the bulky groups into the iridium(III) cation. To evaluate the thermal stability of two ionic complexes, thermogravimetric analysis (TGA) was conducted. As shown in Figure S1, Supporting Information, the two complexes show almost the same onset decomposition temperature of weight loss at 5% (320 °C for **Ir1** and 322 °C for **Ir2**), which implies the complexes have good thermal stability and can sublime under heating.

2.2. Photophysical and Electrochemical Properties

The photophysical properties of the two ionic phosphors were recorded in solution, neat film, and solid states.

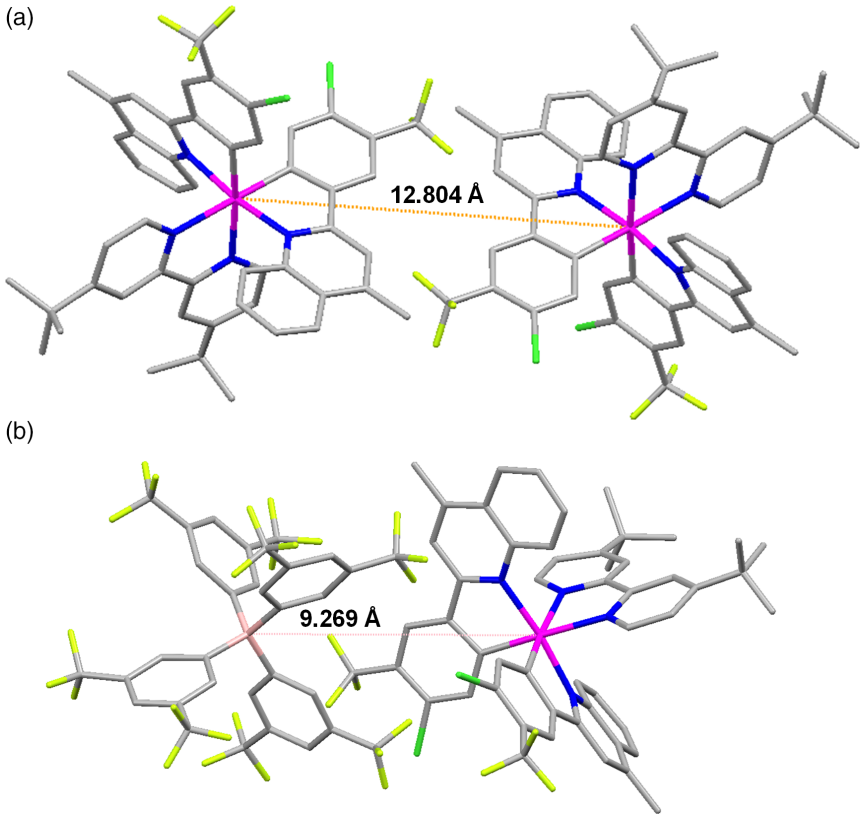

Figure 2. a) The distance between the adjacent metal center of the cations; b) the distance between the adjacent metal center and boron center of the complex **Ir2** in crystals. Note: the carbon atom in gray, iridium atom in scarlet, nitrogen atom in blue, fluorine atom in chartreuse, chlorine atom in green, and boron atom in pink.

The ultraviolet–visible (UV–Vis) absorption spectra and PL spectra were obtained in CH_2Cl_2. It was found that the profiles of absorption and PL spectra (**Figure 3**a) were almost the same for **Ir1** and **Ir2**. The intense absorption from 250 nm to 380 nm should be attributed to the $\pi \rightarrow \pi^*$ transition of the cyclometalated ligand of the complexes.[5,28] The weak absorption from 380 to 550 nm can be attributed to the metal-to-ligand charge-transfer transition because of the strong spin–orbit coupling between the singlet and triplet excited states.[5a,28] At room temperature, an intense yellow phosphorescence of the ionic phosphors in CH_2Cl_2 can be observed (Figure 3a). Both complexes show the same emission spectra with the wavelength of 538 and 570 nm (as the emission shoulder) in CH_2Cl_2. Notably, the extremely broad FWHM for those yellow complexes (100 nm) is realized. The Φ_{PL} of the ionic phosphors were obtained by using an integrating sphere in the Ar-saturated CH_2Cl_2. The Φ_{PL} of ionic phosphors were 0.98 for **Ir1** and 0.91 for **Ir2**, which imply that the steric hindrance from the substituents in the ligands and the bulky counterion can effectively suppress the triplet–triplet annihilation of iridium(III) cations. In the Ar-saturated CH_2Cl_2, the room temperature lifetimes (Figure 3c) of the iridium(III) phosphors were 2.15 μs for **Ir1** and 1.98 μs for **Ir2**, indicating the phosphorescent nature of radiative transition. The alkyl group on the ancillary ligands can have an impact on the excited-state dynamics of the complexes. Based on the observed lifetime and Φ_{PL}, nonradiative decay rates (k_{nr}) and radiative decay rates (k_r) of both complexes can be calculated. As shown in **Table 1**, although the complexes show the same k_r of $4.6 \times 10^5\ s^{-1}$, the k_{nr} of **Ir2** ($4.5 \times 10^4\ s^{-1}$) is much larger than that of **Ir1** ($9.3 \times 10^3\ s^{-1}$), indicating that the free rotation of *tert*-butyl on **Ir2** in CH_2Cl_2 can improve the nonradiative decay rates. Low-temperature (77 K) phosphorescence spectra (Figure 3b) of complexes **Ir1** and **Ir2** were recorded in 2-methyltetrahydrofuran (2–MeTHF). Slightly different from the PL spectra at room temperature, the phosphorescence spectra at 77 K display a blueshift and the vibronic bands with fine structures. Both complexes exhibited the rigidochromic shifts of 11 nm (Table S2, Supporting Information). The triplet energies (T_1) of the two phosphors (Table 1) can be estimated by the highest-energy vibronic subband in the low-temperature phosphorescence spectra. The phosphors share the same T_1 energy (2.35 eV for **Ir1** and **Ir2**).

The photophysical properties of the two phosphors were also explored in neat films and solid states. Because of the bulky groups and counter ions in the complexes, the emission spectra of two phosphors are also similar and show the monomolecular emission both in neat films (**Figure 4**a) and solid states (Figure 4b). Photographs of the two complexes under sunlight and 365 nm UV light are shown in Figure 4b. The detailed emission properties of the two complexes in neat films and solid states

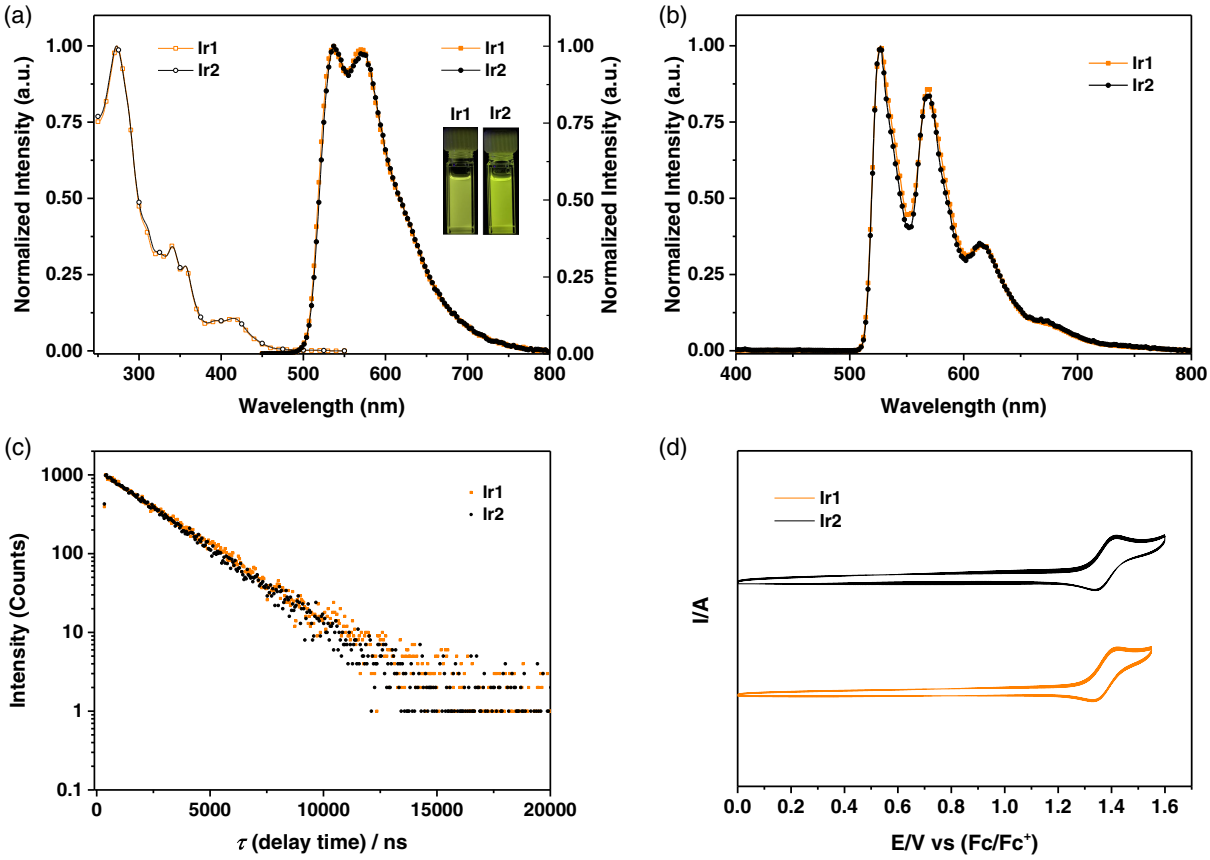

Figure 3. a) UV–vis absorption and PL spectra of **Ir1** and **Ir2** at room temperature in the Ar-saturated CH_2Cl_2; b) PL spectra of **Ir1** and **Ir2** at 77 K in 2-MeTHF; c) phosphorescent decay curves of **Ir1** and **Ir2** in the Ar-saturated CH_2Cl_2 at 298 K; d) cyclic voltammograms of **Ir1** and **Ir2** under a scan rate of 100 mV s^{-1} in the N_2-saturated CH_3CN. Inset: Luminescence photographs of the complexes in CH_2Cl_2.

Table 1. Photophysical and electrochemical properties for **Ir1** and **Ir2**.

Complex	Emission in CH_2Cl_2[a]						E_{onset}^{ox} [eV][b]	E_g [eV][c]	T_1 [eV][d]	HOMO/LUMO [eV][c]
	λ_{em} [nm]	FWHM [nm]	τ [μs]	Φ_{PL}	k_r [s^{-1}]	k_{nr} [s^{-1}]				
Ir1	538, 570 (sh)	100	2.15	0.98	4.6×10^5	9.3×10^3	1.30	2.30	2.35	−6.10/−3.80
Ir2	538, 570 (sh)	100	1.98	0.91	4.6×10^5	4.5×10^4	1.30	2.30	2.35	−6.10/−3.80

[a]At a concentration of 1.0×10^{-5} mol L^{-1} in the Ar-saturated CH_2Cl_2, $\lambda_{ex} = 365$ nm, at 25 °C; [b]In CH_2Cl_2; [c]HOMO (eV) $= -e(E_{onset}^{ox} + 4.8)$, $E_g = 1240/\lambda$, LUMO (eV) $= E_g +$ HOMO; [d]the triplet energy (T_1) was calculated from the highest-energy vibronic subband of the phosphorescence spectrum at a concentration of 1.0×10^{-5} mol L^{-1} in 2-MeTHF at 77 K, $\lambda_{ex} = 365$ nm.

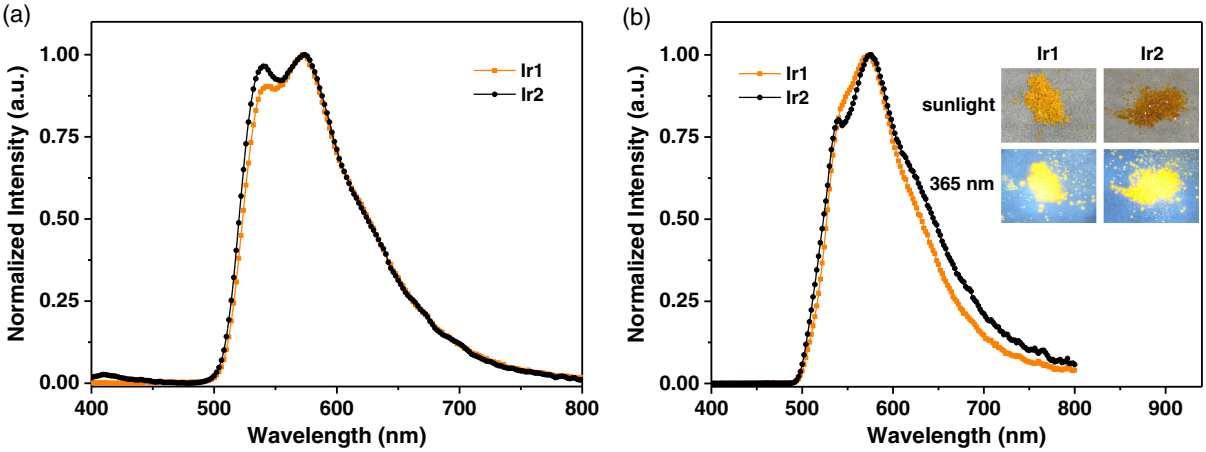

Figure 4. a,b) PL spectra of **Ir1** and **Ir2** in neat film and the solid states at 298 K. Inset: Photographs of the complexes under sunlight and 365 nm UV light.

are listed in Table S3, Supporting Information. The FWHMs of both complexes (102 nm in neat film and 104 nm in solid for **Ir1**; 106 nm in neat film and 122 nm in solid for **Ir2**) are slightly broader than those in solution due to the weak intermolecular interactions. The lifetimes of the two complexes are smaller than those in solution. For complex **Ir1**, the lifetimes are 1.07 μs ($\tau_1 = 0.72$ μs (47%), $\tau_2 = 1.38$ μs (53%)) in neat film and 1.49 μs in solid (Figure S2 and S3, Supporting Information), whereas for complex **Ir2**, the lifetimes are 1.51 μs ($\tau_1 = 0.41$ μs (5%), $\tau_2 = 1.57$ μs (95%)) in neat film and 1.37 μs in solid. It should be noted that Φ_{PL} of the two complexes (0.16 in neat film and 0.15 in solid for **Ir1**; 0.12 in neat film and 0.13 in solid for **Ir2**) in both neat films and solid states are much smaller than those in solutions. The decrease in Φ_{PL} of the complexes in neat films and solid states indicates the presence of the triplet–triplet annihilation in condensed states.[30]

The electrochemical properties of the two phosphors were then investigated using cyclic voltammetry in the N_2-saturated CH_3CN. The phosphors display reversible waves in the oxidation process (Figure 3d), which is originated from the oxidation of metal center in the iridium(III) cation.[5a] The oxidation potentials are the same for the two phosphors (1.30 eV for **Ir1** and **Ir2**). Based on the oxidation potentials of the phosphors, the energy level of the highest occupied molecular orbital (HOMO) of both phosphors can be calculated to be −6.10 eV, and the energy level of the lowest unoccupied molecular orbital (LUMO) of the phosphors is −3.80 eV, as deduced from $E_g +$ HOMO.

Theoretical calculations for complexes **Ir1** and **Ir2** were also conducted by Gaussian 09 package to better understand the photophysical behaviors of the ionic phosphors.[31] As shown in **Figure 5**, the electron cloud distributions and energy levels

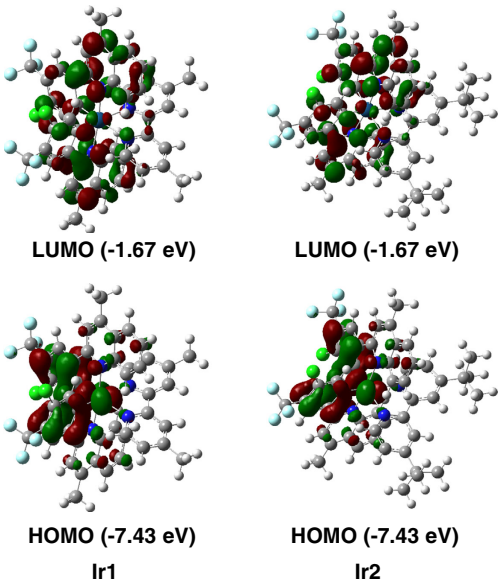

Figure 5. The electron cloud distributions and energy levels of HOMOs and LUMOs of **Ir1** and **Ir2** at T_1 state.

of the ionic phosphors at the triplet state were calculated. For both phosphors, the HOMOs are mostly located in the chlorinated phenyl units and metal center, whereas the LUMOs are mostly distributed in the quinoline units, consistent with the previous result.[4c] According to the calculations, the two triplet excited states of **Ir1** and **Ir2** are both derived from mixed ^{3}MLCT, ^{3}ILCT, and LC $^3\pi$–π^* transitions.[23] The calculated energy levels for **Ir1** and **Ir2** are almost the same (−7.43 eV for HOMO and −1.67 eV for LUMO), indicating that the alkyl group (methyl or *tert*-butyl) in the auxiliary ligand almost has no effects on the excited states of these ionic complexes. The calculated emission wavelengths from the first triplet energy level are 539.48 nm for **Ir1** and 539.52 nm for **Ir2**, which is also consistent with the triplet energies of complexes measured at the low temperature.

2.3. Yellow Organic Light-Emitting Diodes

Ir1 and **Ir2** were further used to evaluate their electroluminescent properties by vacuum thermal evaporation method. The yellow OLEDs were fabricated with the device structures of the indium tin oxide (ITO)/molybdenum trioxide (MoO_3) (3 nm)/di-[4-(*N*,*N*-ditolylamino)-phenyl] cyclohexane (TAPC) (40 nm)/4,4′-bis(9*H*-carbazol-9-yl)biphenyl (CBP): *x* wt% emitter (20 nm)/1,3,5-tri(m-pyrid-3-yl-phenyl)benzene (TmPyPb) (50 nm)/lithium fluoride (LiF) (1 nm)/aluminum (Al) (100 nm). As shown in Figure S4, Supporting Information, the ITO acts as the anode, MoO_3 acts as the hole injection layer (HIL), TAPC acts as the hole-transporting layer (HTL), CBP layer doped with iridium(III) complex acts as the emissive layer, TmPyPb acts as the electron-transporting layer (ETL), a 1 nm LiF layer, and a 100 nm Al act as the cathode layer. The energy diagrams for the yellow OLEDs are shown in Figure S4, Supporting Information. The iridium(III) complexes with 5 and 10 wt% doping concentration in CBP served as the emissive layers. The devices based on **Ir1** are denoted by Y1, and the devices based on **Ir2** are denoted by Y2. From the energy level diagrams of OLEDs (Figure S4, Supporting Information), the LUMO/HOMO levels of the iridium(III) emitters are within the host material CBP. So, good charge carrier trapping in these devices is realized.[32] In addition, because of the large energy gap (0.5 eV) between the HOMO of TmPyPb and the HOMO of CBP, electrons and holes are expected to be well confined within the doped emissive layer.[33–35]

The electroluminescence spectra, current density (*J*)–voltage (*V*)–luminance (*L*), power efficiency (*PE*)–*L*, and current efficiency (*CE*)–*L*–*EQE* curves of the devices are shown in **Figure 6**. The prepared devices display an intense yellow light with the EL peak at 572 nm for complex **Ir1** and 576 nm for complex **Ir2**, respectively. The EL spectra of the devices, as shown in Figure 6a, show dominant emission bands originating from the iridium(III) phosphors without other residual emission arising from the other layers or host material, implying that

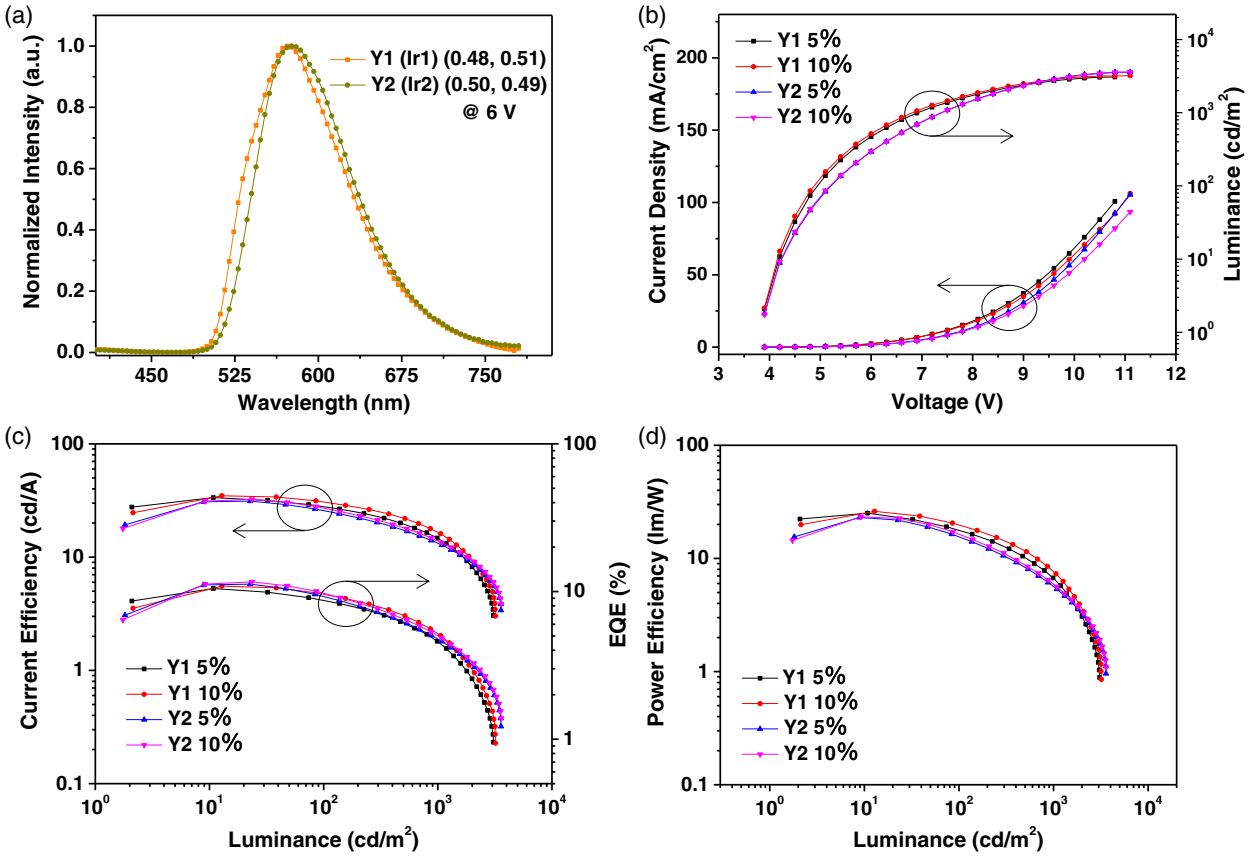

Figure 6. a) Normalized EL spectra, b) *J*–*V*–*L*, c) *CE*–*L*–*EQE*, and d) *PE*–*L* curves for the yellow OLEDs Y1 and Y2 with 5% and 10% doping concentration.

excitons formed within the emissive layer deactivate by the phosphorescence emission of the phosphors. It should be noted that the emission spectra of the OLEDs are slightly different from those of the complexes in the solution or solid states. These variations in emission spectra may be the results of the different intermolecular interactions of the complexes.[2b,36] The CIE coordinates for the OLEDs ((0.48, 0.51) for Y1, (0.50, 0.49) for Y2) are in the yellow region of the CIE chromaticity diagram. It is highlighted that all yellow devices display extremely broad emission band (FWHMs of 105 nm for Y1 and 99 nm for Y2), which is comparable to or broader than those of the reported ones.[5a,9–12,14,15,28]

As shown in **Table 2**, the yellow OLEDs based on the new ionic iridium(III) complexes show decent EL performances. The prepared OLEDs show relatively low turn-on voltages ($V_{turn\text{-}on}$) ranging from 3.5 to 3.9 V. The maximum luminance of the OLEDs ranges from 3073 to 3599 cd m^{-2}. The peak *CE*, *PE*, and *EQE* of the devices based on **Ir1** and **Ir2** are in the range of 31.2–34.8 cd A^{-1}, 23.0–26.1 lm W^{-1}, and 10.5–11.6%, respectively. The maximum *EQE* of Y2 based on **Ir2** is slightly higher than that of Y1 based on **Ir1**. It is found that the device performance is almost independent on the doping concentration, which is probably the result of the steric hindrance from the bulky counter ions and the methyl/trifluoromethyl moieties in the ligands. The obtained EL performances are comparable or even superior to most of the devices based on ionic iridium(III) complexes showing similar emission band.[24,27,37] Although the device performance of ionic iridium(III) complex is far behind that of the neutral one, we believe that they would be further improved by the smart molecular design or the device structure optimization in the future study.

2.4. White Organic Light–Emitting Diodes

Complex **Ir2** was used to prepare the two-color-based white device to further demonstrate its use in white electroluminescence. As shown in Figure S5, Supporting Information, the white OLED (W) has the device structure of ITO/MoO_3 (3 nm)/4,4′,4"-tris(carbazol-9-yl)triphenylamine (TCTA) (40 nm)/bis(2-(2-hydroxyphenyl)-pyridine) beryllium ($Bepp_2$) (5 nm)/**Ir2** (0.03 nm)/$Bepp_2$ (5 nm)/1,3,5-tris(1-phenyl–1*H*-benzimidazol-2-yl)benzene (TPBi) (50 nm)/LiF (1 nm)/Al (100 nm), where MoO_3, TCTA, and TPBi serve as the HIL, HTL, and ETL, respectively. To obtain white light emission, an ultrathin yellow emissive layer (0.03 nm) of **Ir2** was introduced into the blue emissive layer (10 nm) of $Bepp_2$. As shown in Figure S5, Supporting Information, the LUMO, HOMO, and triplet energy levels of **Ir2** are all within those of $Bepp_2$, which is in favor of the energy transfer.[4c] Due to the ultrathin doping of **Ir2**, the incomplete energy transfer from the blue emissive $Bepp_2$ to yellow emissive **Ir2** will be expected to occur, and give rise to the complementary-color-based white spectrum.[4c] The normalized spectra of EL, *J–V–L*, *PE–L*, and *CE–L–EQE* curves for the white OLED are shown in **Figure 7**, S6, and S7, Supporting Information, and the device performance is listed in Table 2. The white OLED showed a low

Table 2. Device performances of the monochromic and white OLEDs.

Device	*x*%	λ_{EL} [nm]	CIE (*x*, *y*)[a)]	V_{ON}[b)] [V]	L_{max} [cd m^{-2}]	CE_{max} [cd A^{-1}]	PE_{max} [lm W^{-1}]	EQE_{max}	FWHM [nm]
Y1	5	572	(0.48, 0.51)	3.5	3073	33.6	25.1	10.5	105
Y1	10	572	(0.48, 0.51)	3.6	3202	34.8	26.1	10.9	105
Y2	5	576	(0.50, 0.49)	3.8	3580	31.2	23.0	11.2	99
Y2	10	576	(0.50, 0.49)	3.9	3599	32.4	23.4	11.6	99
W	–	442, 556	(0.29, 0.31)	3.1	4733	26.2	24.9	9.2	–

[a)]At 6 V for yellow device, and at 8 V for white device; [b)]luminance is 1 cd.m^{-2}.

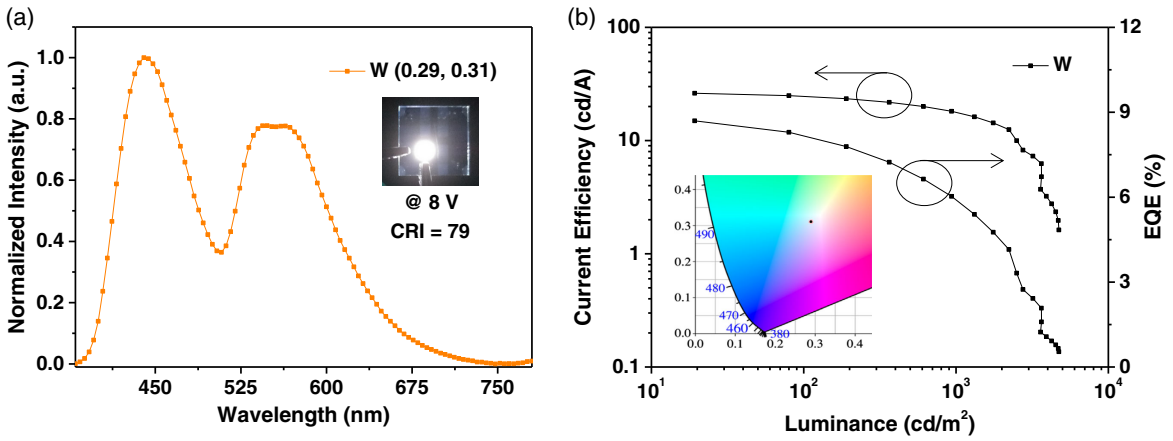

Figure 7. a) Normalized EL spectra and b) *CE–L–EQE* curves for the white OLED. The insets show the photograph (left) and the 1931 CIE coordinate (right) of the white OLED at 8 V.

operation voltage of 3.1 V. By applying a voltage, two emission bands from $Bepp_2$ and **Ir2** can be observed. At 8 V, the emission spectrum showed the balanced emission bands with brightness of 4241 cd m^{-2}, 1931 CIE coordinate of (0.29, 0.31), and CRI of 79, which meets the requirements for the practical lighting. It should be noted that the white spectra vary with the applied voltages because of the unbalanced recombination of carriers within the **Ir2** and $Bepp_2$ layers, which may be further improved by optimizing the device architecture. In addition, the white device gave the maximum *CE*, *PE*, and *EQE* of 26.2 cd A^{-1}, 24.9 lm W^{-1}, and 9.2%, respectively. The results suggest that the synthesized yellow ionic iridium(III) phosphors will show great potentials for high-performance solid state lighting.

3. Conclusion

In conclusion, by incorporation of chlorine-modified 2-phenylquinoline ligand and introduction of bulky counter ion, we designed and prepared two efficient yellow ionic iridium(III) emitters featuring excellent sublimation ability. Due to the presence of bulky counter ion, these ionic iridium(III) complexes exhibit intense yellow phosphorescence in both solution and solid states. They show the same emission wavelength (538 and 573 nm as the emission shoulder) with quite high quantum yields (up to 0.91) in the Ar-saturated dichloromethane at room temperature. Notably, by taking advantage of the same intensities of emission maximum and shoulder, these complexes also exhibit very broad emission band (as high as 100 nm), providing a great potential in realizing solid-state lighting. The as-prepared OLEDs show yellow phosphorescence with broad emission band up to 105 nm, and the peak *EQE* of 11.6% was realized for the yellow OLEDs. Finally, the complementary-color-based white OLED was realized by incorporating complex **Ir2**. The as-prepared white OLED showed peak *EQE* of 9.2%, the 1931 CIE coordinate of (0.29, 0.31), and CRI of 79. These preliminary results reveal that such new ionic iridium(III) complexes show a good promise for the future development of high-performance monochromic and white electroluminescence.

4. Experimental Section

The related information on material characterization, device fabrication, and performance testing can be found in the Supporting Information.

Synthesis of Ionic Iridium(III) Complexes: A mixture of the chloro-bridged dimer (0.1 mmol) and 4,4′-dimethyl-2,2′-bipyridine or 4,4′-di-*tert*-butyl-2,2′-bipyridine (0.22 mmol) was dispersed in the solvent of CH_2Cl_2 (30 mL) and methanol (10 mL), and the mixture was stirred at 50 °C for 8 h under N_2. After the reaction was complete, the solvent was removed under reduced pressure. Then, the solid obtained was dissolved in methanol (20 mL). The sodium tetrakis[3,5-bis(trifluoromethyl)phenyl] borate (0.2 mmol) in H_2O (10 mL) was added into the previous methanol solution under stirring. Finally, the solvent was removed under reduced pressure. The crude product was purified by column chromatography (*n*-hexane/dichloromethane as eluent) to give the final ionic iridium(III) complex.[23]

Ir1: Yellow powder (81% yield). ^{1}H NMR (400 MHz, $CDCl_3$, δ): 8.27 (s, 2H), 8.01 (s, 2H), 7.96 (d, $J = 5.72$ Hz, 2H), 8.85 (d, $J = 8.28$ Hz, 2H), 7.67 (s, 8H), 7.59 (s, 2H), 7.43 (s, 4H), 7.34 (t, $J = 7.44$ Hz, 2H), 7.20 (d, $J = 5.96$ Hz, 2H), 7.17 (d, $J = 8.96$ Hz, 2H), 6.98 (d, $J = 8.24$ Hz, 2H), 6.56 (s, 2H), 2.89 (s, 6H), 2.27 (s, 6H). ^{19}F{^{1}H} NMR (376 MHz, $CDCl_3$, δ): −68.25 (s); −68.59 (s). matrix-assisted laser desorption/ionization time-of-flight mass (MALDI–TOF–MS) (m/z): calcd for $C_{46}H_{32}Cl_2F_6IrN_4^+$ (the cation of **Ir1**), 1017.154; found, 1017.162.

Ir2: Yellow powder (83% yield). ^{1}H NMR (400 MHz, CD_3CN, δ): 8.50 (s, 2H), 8.34 (s, 2H), 8.09 (d, $J = 5.96$ Hz, 2H), 8.02–8.00 (m, 4H), 7.71 (s, 8H), 7.68 (s, 4H), 7.51–7.46 (m, 4H), 7.25 (d, $J = 8.84$ Hz, 2H), 7.06 (ddd, $J = 8.24$ Hz, $J = 7.28$ Hz, $J = 0.96$ Hz, 2H), 6.70 (s, 2H), 2.91 (s, 6H), 1.28 (s, 18H). ^{19}F{^{1}H} NMR (376 MHz, CD_3CN, δ): −68.34, −69.38. MALDI–TOF–MS (*m/z*): calcd for $C_{52}H_{44}Cl_2F_6IrN_4^+$ (the cation of **Ir2**), 1101.248; found, 1101.279.

Supporting Information

Supporting Information is available from the Wiley Online Library or from the author.

Acknowledgements

P.T. and X.K.Z. contributed equally to this work. The authors acknowledge the National Natural Science Foundation of China (61905120, 51873176, and 61705156), National Funds for Distinguished Young Scientists (61825503), Start-up Fund for RAPs under the Strategic Hiring Scheme (P0035922), the Hong Kong Research Grants Council (PolyU 153058/19P), the Hong Kong Polytechnic University (1–ZE1C), Ms. Clarea Au for the Endowed Professorship in Energy (847S), Research Institute for Smart Energy (RISE), Natural Science Foundation of Jiangsu Province of China (BK20190740), and Key R&D program of Shanxi Province (International Cooperation, 201903D421087) for financial support.

Conflict of Interest

The authors declare no conflict of interest.

Data Availability Statement

Research data are not shared.

Keywords

broad emission, ionic iridium(III) complexes, sublimable ionic complexes, yellow phosphorescence

Received: April 23, 2021
Revised: June 29, 2021
Published online: September 21, 2021

[1] a) X. Yang, G. Zhou, W.-Y. Wong, *Chem. Soc. Rev.* **2015**, *44*, 8484; b) A. Haque, L. Xu, R. A. Al-Balushi, M. K. Al-Suti, R. Ilmi, Z. Guo, M. S. Khan, W.-Y. Wong, P. R. Raithby, *Chem. Soc. Rev.* **2019**, *48*, 5547; c) V. W. W. Yam, V. K. M. Au, S. Y. L. Leung, *Chem. Rev.* **2015**, *115*, 7589; d) J. Lee, H.-F. Chen, T. Batagoda, C. Coburn, P. I. Djurovich, M. E. Thompson, S. R. Forrest, *Nat. Mater.* **2016**, *15*, 92.

[2] a) P. Tao, S.-J. Liu, W.-Y. Wong, *Adv. Opt. Mater.* **2020**, *8*, 2000985; b) P. Tao, Y. Miao, H. Wang, B. Xu, Q. Zhao, *Chem. Rec.* **2019**, *19*, 1531; c) J.-S. Huh, M. J. Sung, S.-K. Kwon, Y.-H. Kim, J.-J. Kim, *Adv. Funct. Mater.* **2021**, *31*, 2100967.

[3] a) P. Ganesan, W.-Y. Hung, J.-Y. Tso, C.-L. Ko, T.-H. Wang, P.-T. Chen, H.-F. Hsu, S.-H. Liu, G.-H. Lee, P.-T. Chou, A. K.-Y. Jen, Y. Chi, *Adv. Funct. Mater.* **2019**, *29*, 1900923; b) Y. Yuan, J.-L. Liao,

S.-F. Ni, Al. K.-Y. Jen, C.-S. Lee, Y. Chi, *Adv. Funct. Mater.* **2020**, *30*, 1906738; c) S. F. Wang, Y. Yuan, Y.-C. Wei, W.-H. Chan, L.-W. Fu, B.-K. Su, I-Y. Chen, K.-J. Chou, P.-T. Chen, H.-F. Hsu, C.-L. Ko, W.-Y. Hung, C.-S. Lee, P.-T. Chou, Y. Chi, *Adv. Funct. Mater.* **2020**, *30*, 2002173.

[4] a) W.-C. Chen, C. Sukpattanacharoen, W.-H. Chan, C.-C. Huang, H.-F. Hsu, D. Shen, W.-Y. Hung, N. Kungwan, D. Escudero, C.-S. Lee, Y. Chi, *Adv. Funct. Mater.* **2020**, *30*, 2002494; b) X. Li, J. Zhang, Z. Zhao, L. Wang, H. Yang, Q. Chang, N. Jiang, Z. Liu, Z. Bian, W. Liu, Z. Lu, C. Huang, *Adv. Mater.* **2018**, *30*, 1705005; c) Y. Miao, P. Tao, K. Wang, H. Li, B. Zhao, L. Gao, H. Wang, B. Xu, Q. Zhao, *ACS Appl. Mater. Interfaces* **2017**, *9*, 37873.

[5] a) P. Tao, W.-L. Li, J. Zhang, S. Guo, Q. Zhao, H. Wang, B. Wei, S.-J. Liu, X.-H. Zhou, Q. Yu, B.-S. Xu, W. Huang, *Adv. Funct. Mater.* **2016**, *26*, 881; b) P. Tao, Y. Zhang, J. Wang, L. Wei, H. Li, X. Li, Q. Zhao, X. Zhang, S. Liu, H. Wang, W. Huang, *J. Mater. Chem. C* **2017**, *5*, 9306; c) Y. Miao, P. Tao, L. Gao, X. Li, L. Wei, S. Liu, H. Wang, B. Xu, Q. Zhao, *J. Mater. Chem. C* **2018**, *6*, 6656; d) E. Baranoff, B. F. E. Curchod, *Dalton Trans.* **2015**, *44*, 8318; e) Y. Zheng, A. S. Batsanov, R. M. Edkins, A. Beeby, M. R. Bryce, *Inorg. Chem.* **2012**, *51*, 290; f) V. Sivasubramaniam, F. Brodkorb, S. Hanning, H. P. Loebl, V. Elsbergen, H. Boerner, U. Scherf, M. Kreyenschmidt, *J. Fluorine Chem.* **2009**, *130*, 640.

[6] C. Fan, C.-L. Yang, *Chem. Soc. Rev.* **2014**, *43*, 6439.

[7] S. Chen, G. Tan, W. Wong, H. Kwok, *Adv. Funct. Mater.* **2011**, *21*, 3785.

[8] Z. S. Zhang, S. Z. Yue, Y. K. Wu, P. R. Yan, Q. Y. Wu, D. L. Qu, S. Y. Liu, Y. Zhao, *Opt. Express* **2014**, *22*, 1815.

[9] S. L. Lai, S. L. Tao, M. Y. Chan, T. W. Ng, M. F. Lo, C. S. Lee, X. H. Zhang, S. T. Lee, *Org. Electron.* **2010**, *11*, 1511.

[10] Y. L. Chang, B. A. Kamino, Z. B. Wang, M. G. Helander, Y. L. Rao, L. Chai, S. N. Wang, T. P. Bender, Z. H. Lu, *Adv. Funct. Mater.* **2013**, *23*, 3204.

[11] D. M. Kang, J. W. Kang, J. W. Park, S. O. Jung, S. H. Lee, H. D. Park, Y. H. Kim, S. C. Shin, J. J. Kim, S. K. Kwon, *Adv. Mater.* **2008**, *20*, 2003.

[12] S. L. Lai, S. L. Tao, M. Y. Chan, M. F. Lo, T. W. Ng, S. T. Lee, W. M. Zhao, C. S. Lee, *J. Mater. Chem.* **2011**, *21*, 4983.

[13] S. H. Ye, T. Q. Hu, Z. Zhou, M. Yang, M. H. Quan, Q. B. Mei, B. C. Zhai, Z. H. Jia, W. Y. Lai, W. Huang, *Phys. Chem. Chem. Phys.* **2015**, *17*, 8860.

[14] F. Dumur, M. Lepeltier, H. Z. Siboni, D. Gigmes, H. Aziz, *Adv. Opt. Mater.* **2014**, *2*, 262.

[15] J. H. Jou, Y. X. Lin, S. H. Peng, C. J. Li, Y. M. Yang, C. L. Chin, J. J. Shyue, S. S. Sun, M. Lee, C. T. Chen, M. C. Liu, C. C. Chen, G. Y. Chen, J. H. Wu, C. H. Li, C. F. Sung, M. J. Lee, J. P. Hu, *Adv. Funct. Mater.* **2014**, *24*, 555.

[16] Q. Zhao, C. Huang, F. Li, *Chem. Soc. Rev.* **2011**, *40*, 2508.

[17] R. Bai, X. Meng, X. Wang, L. He, *Adv. Funct. Mater.* **2020**, *30*, 1907169.

[18] R. Bai, X. Meng, X. Wang, L. He, *Adv. Funct. Mater.* **2021**, *31*, 2007167.

[19] Q. Yu, T. Huang, Y. Li, H. Wei, S. Liu, W. Huang, J. Du, Q. Zhao, *Chem. Commun.* **2017**, *53*, 4144.

[20] J. Zhao, K. Yan, G. Xu, X. Liu, Q. Zhao, C. Xu, S. Gou, *Adv. Funct. Mater.* **2020**, *31*, 2008325.

[21] W.-Y. Wong, G.-J. Zhou, X.-M. Yu, H.-S. Kwok, Z. Lin, *Adv. Funct. Mater.* **2007**, *17*, 315.

[22] D. Ma, L. Duan, Y. Wei, L. He, L. Wang, Y. Qiu, *Chem. Commun.* **2014**, *50*, 530.

[23] D. Ma, R. Liu, C. Zhang, Y. Qiu, L. Duan, *ACS Photonics* **2018**, *5*, 3428.

[24] D. Ma, T. Tsuboi, Y. Qiu, L. Duan, *Adv. Mater.* **2017**, *29*, 1603253.

[25] R. Liu, D. Ma, L. Duan, *J. Mater. Chem. C* **2020**, *8*, 14766.

[26] a) D. Ma, Y. Qiu, L. Duan, *Adv. Funct. Mater.* **2016**, *26*, 3438; b) L. He, L. Duan, J. Qiao, D. Zhang, L. Wang, Y. Qiu, *Org. Electron.* **2010**, *11*, 1185; c) D. Ma, C. Zhang, Y. Qiu, L. Duan, *Org. Electron.* **2016**, *39*, 16.

[27] a) D. Ma, L. Duan, *Chem. Rec.* **2019**, *19*, 1483; b) R. Bai, X. Meng, X. Wang, L. He, *Adv. Funct. Mater.* **2020**, *30*, 1907169; c) R. Bai, X. Meng, X. Wang, L. He, *Adv. Funct. Mater.* **2021**, *31*, 2007167; d) H.-C. Su, Y.-R. Chen, K.-T. Wong, *Adv. Funct. Mater.* **2020**, *30*, 1906898.

[28] P. Tao, X.-K. Zheng, X.-Z. Wei, M.-T. Lau, Y.-K. Lee, Z.-K. Li, Z.-L. Guo, F.-Q. Zhao, X. Liu, S.-J. Liu, Q. Zhao, Y.-Q. Miao, W.-Y. Wong, *Mater. Today Energy* **2021**, *21*, 100773.

[29] a) J. Qu, H. Chen, J. Zhou, H. Lai, T. Liu, P. Chao, D. Li, Z. Xie, F. He, Y. Ma, *ACS Appl. Mater. Interfaces* **2018**, *10*, 39992; b) H. Yao, J. Wang, Y. Xu, S. Zhang, J. Hou, *Acc. Chem. Res.* **2020**, *53*, 822.

[30] a) Q. Zhao, L. Li, F. Li, M. Yu, Z. Liu, T. Yi, C. Huang, *Chem. Commun.* **2008**, 685. b) H. Wu, T. Yang, Q. Zhao, J. Zhou, C. Li, F. Li, *Dalton Trans.* **2011**, *40*, 1969.

[31] M. J. Frisch, G. W. Trucks, H. B. Schlegel, G. E. Scuseria, M. A. Robb, J. R. Cheeseman, G. Scalmani, V. Barone, B. Mennucci, G. A. Petersson, H. Nakatsuji, M. Caricato, X. Li, H. P. Hratchian, A. F. Izmaylov, J. Bloino, G. Zheng, J. L. Sonnenberg, M. Hada, M. Ehara, K. Toyota, R. Fukuda, J. Hasegawa, M. Ishida, T. Nakajima, Y. Honda, O. Kitao, H. Nakai, T. Vreven Jr., J. A. Montgomery, et al., *Gaussian09, Revision B.01*, Gaussian Inc., Wallingford, CT, **2010**.

[32] J. Xue, L. Xin, J. Hou, L. Duan, R. Wang, Y. Wei, J. Qiao, *Chem. Mater.* **2017**, *29*, 4775.

[33] S.-J. Su, T. Chiba, T. Takeda, J. Kido, *Adv. Mater.* **2008**, *20*, 2125.

[34] Y.-H. Chen, F.-C. Zhao, Y.-B. Zhao, J.-S. Chen, D.-G. Ma, *Org. Electron.* **2012**, *13*, 2807.

[35] P. Tao, Y. Miao, Y. Zhang, K. Wang, H. Li, L. Li, X. Li, T. Yang, Q. Zhao, H. Wang, S. Liu, X. Zhou, B. Xu, W. Huang, *Org. Electron.* **2017**, *45*, 293.

[36] Q. Li, C. Shi, M. Huang, X. Wei, H. Yan, C. Yang, A. Yuan, *Chem. Sci.* **2019**, *10*, 3257.

[37] F. Zhang, Y. Guan, S. Wang, S. Li, F. Zhang, Y. Feng, S. Chen, G. Cao, B. Zhai, *Dyes Pigments* **2016**, *130*, 1.